

# Compressing Transformer Language Models via Matrix Product Operator Decomposition

A Case Study on PicoGPT

Younes Javanmard<sup>1</sup>, Tanmoy Pandit<sup>2</sup>, and Masoud Mardani<sup>3</sup>

<sup>1</sup>Institut für Theoretische Physik, Leibniz Universität Hannover, Appelstraße 2, 30167 Hannover, Germany,  
younes.javanmard@itp.uni-hannover.de

<sup>2</sup>VTT Technical Research Centre of Finland, Tietotie 3, Espoo, Finland,

<sup>3</sup>National High Magnetic Field Laboratory, Tallahassee, FL 32310, USA,

March 31, 2026

## Abstract

**Background.** Transformer-based language models achieve state-of-the-art performance across natural language tasks, but their quadratic parameter scaling with hidden dimension makes deployment on resource-constrained hardware expensive. Existing compression methods — including pruning, quantization, and low-rank factorization — treat all weight structures uniformly and offer limited control over the approximation error. Matrix Product Operator (MPO) decomposition, a tensor network technique originally developed for quantum many-body simulations, provides a principled alternative: it factorizes weight matrices into chains of low-rank cores whose approximation quality is governed by a single interpretable hyperparameter, the bond dimension  $\chi$ .

**Methods.** We replace every `nn.Linear` layer in PicoGPT — a GPT-2-style character-level language model with  $\sim 1$  M parameters — with an `MPOLinear` module whose weight is parameterised as an MPO chain. Cores are initialized either via the TT-SVD algorithm applied to pretrained dense weights or from random initialisations. All cores are stored as standard `nn.Parameter` tensors; gradient flow through the `tensorcontraction` chain is handled automatically by PyTorch autograd, requiring no custom backward pass. We derive balanced factorization schemes for each of the five distinct weight shapes in PicoGPT and evaluate bond dimensions  $\chi \in \{4, 8, 16, 32\}$  on the Tiny Shakespeare corpus.

**Results.** MPO compression achieves up to  $13\times$  parameter compression per transformer block at  $\chi = 4$ . At  $\chi = 16$  — with 191 872 parameters versus the dense baseline of 1 020 224 — the model retains 97.7% of the baseline token accuracy (51.6% vs. 52.8%), a gap of 1.2 percentage points. Per-layer reconstruction error decreases systematically with increasing bond dimension and is consistently lower for three-site ( $L = 3$ ) factorisations than for two-site ( $L = 2$ ) ones at the same  $\chi$ . Under the parameter-efficiency proxy used in this work, the MPO model at  $\chi = 8$  attains the highest score.

**Conclusions.** MPO compression provides a theoretically grounded and practically accessible route to transformer parameter compression with explicit control over the accuracy–compression trade-off. Our open-source PyTorch implementation is fully compatible with standard training pipelines and requires no modifications to the model training loop. Our current implementation demonstrates parameter compression and training compatibility; realising inference-time memory and FLOP savings will require direct structured contractions that avoid reconstructing the dense weight. These results suggest that MPO parameterization is a promising alternative to standard low-rank and tensor-factorized compression approaches, particularly when interpretable compression control and quantum-physics-motivated analysis are desired.

**Keywords:** tensor networks, matrix product operators, transformer compression, neural network compression, TT-SVD, bond dimension, language models, PyTorch

# Contents

<b>1</b>	<b>Introduction</b>	<b>2</b>
<b>2</b>	<b>Background</b>	<b>3</b>
2.1	Tensor Train and Matrix Product Operators . . . . .	3
2.2	TT-SVD Algorithm . . . . .	4
2.3	Gradient Flow Through MPO Layers . . . . .	4
<b>3</b>	<b>Architecture and Implementation</b>	<b>5</b>
3.1	PicoGPT Architecture . . . . .	5
3.2	MPO Factorisation Schemes . . . . .	5
3.3	The MPOLinear Module . . . . .	6
<b>4</b>	<b>Experimental Setup</b>	<b>6</b>
4.1	Dataset and Tokenisation . . . . .	6
4.2	Training Protocol . . . . .	6
4.3	Compression Modes . . . . .	7
<b>5</b>	<b>Results</b>	<b>7</b>
5.1	Compression Statistics . . . . .	7
5.2	Per-Layer Reconstruction Error . . . . .	8
5.3	Training Dynamics . . . . .	8
5.4	Summary of Results . . . . .	9
<b>6</b>	<b>Discussion</b>	<b>10</b>
<b>7</b>	<b>Conclusion</b>	<b>10</b>
<b>A</b>	<b>Heuristic justification of the MPO initialization scale</b>	<b>12</b>

---

## 1 Introduction

Transformer language models have achieved state-of-the-art performance across a broad range of natural language tasks [Vaswani et al., 2017, Radford et al., 2019, Brown et al., 2020]. However, their parameter counts scale quadratically with the hidden dimension, making deployment on resource-constrained hardware expensive. A key empirical observation motivating compression is that neural network weights are heavily redundant [Denil et al., 2013], suggesting that low-dimensional structure is present. A variety of compression techniques have been proposed, including weight pruning [Han et al., 2015], CP-decomposition of convolutional filters [Lebedev et al., 2015], knowledge distillation [Hinton et al., 2015], and low-rank factorisation [Hu et al., 2022].

An alternative perspective, imported from quantum information theory, represents weight tensors as *Matrix Product Operators* (MPOs) [Oseledets, 2011, Kolda & Bader, 2009, Novikov et al., 2015]. An MPO factorises a high-dimensional weight tensor into a chain of low-rank *cores*, each carrying only  $\mathcal{O}(\chi^2 d^2)$  parameters when the local physical dimensions are of order  $d$  and the bond dimension is  $\chi$ . The bond dimension is the single knob that controls the accuracy–compression trade-off: increasing  $\chi$  systematically recovers the dense weight.

This framework is familiar in the quantum many-body community under the name Tensor Train (TT) [Oseledets, 2011] or Matrix Product State (MPS) when applied to vectors; the operator variant (MPO) is the natural choice for weight matrices. MPO-based neural compression was pioneered by Novikov et al. [2015] for fully-connected layers and subsequently extended to recurrent architectures [Yang et al.,

2017, Tjandra et al., 2017], transformers [Gao et al., 2020], and more recently to large language models by Tomut et al. [2024], who reported substantial compression of LLaMA-2 7B with a relatively modest accuracy drop.

In this paper we apply MPO compression to **PicoGPT** [?], a pedagogical GPT-2-style implementation written from scratch in Julia following the transformer architecture of Vaswani et al. [2017], which we re-implement in PyTorch to enable gradient-based fine-tuning of the compressed cores. The MPO cores are treated as first-class `nn.Parameter` tensors with gradients flowing through the contraction chain automatically — an approach related to the MPO arithmetic framework developed for quantum circuit compilation [Javanmard, 2026]. Our contributions are:

1. A clean, fully autograd-compatible MPO layer (`MPOLinear`) that replaces any `nn.Linear` without custom backward code.
2. Factorisation schemes for all five weight shapes in PicoGPT, derived from balanced MPO design principles.
3. A systematic benchmark comparing dense and MPO-parameterised models across bond dimensions  $\chi \in \{4, 8, 16, 32\}$  on character-level Shakespeare prediction.
4. An analysis of reconstruction error, training dynamics, and the accuracy–compression Pareto frontier.

## 2 Background

### 2.1 Tensor Train and Matrix Product Operators

**Definition 1** (Tensor Train). A tensor  $\mathcal{T} \in \mathbb{R}^{n_1 \times n_2 \times \dots \times n_L}$  is said to be in *Tensor Train* (TT) format with bond dimensions  $(\chi_1, \dots, \chi_{L-1})$  if it can be written as

$$\mathcal{T}_{i_1 i_2 \dots i_L} = \sum_{\alpha_1, \dots, \alpha_{L-1}} \mathcal{A}_{1, i_1, \alpha_1}^{(1)} \mathcal{A}_{\alpha_1, i_2, \alpha_2}^{(2)} \dots \mathcal{A}_{\alpha_{L-1}, i_L, 1}^{(L)}, \quad (1)$$

where  $\mathcal{A}^{(l)} \in \mathbb{R}^{\chi_{l-1} \times n_l \times \chi_l}$  are the *TT-cores*, with boundary conditions  $\chi_0 = \chi_L = 1$ .

**Definition 2** (Matrix Product Operator). A weight matrix  $\mathbf{W} \in \mathbb{R}^{\text{out} \times \text{in}}$  is a *Matrix Product Operator* (MPO) if, after reshaping  $\text{out} = \prod_{l=1}^L d_l^{\text{out}}$  and  $\text{in} = \prod_{l=1}^L d_l^{\text{in}}$ , it can be expressed as

$$W_{(i_1 \dots i_L), (j_1 \dots j_L)} = \sum_{\alpha_1, \dots, \alpha_{L-1}} \mathcal{A}_{1, i_1, j_1, \alpha_1}^{(1)} \mathcal{A}_{\alpha_1, i_2, j_2, \alpha_2}^{(2)} \dots \mathcal{A}_{\alpha_{L-1}, i_L, j_L, 1}^{(L)}, \quad (2)$$

where  $\mathcal{A}^{(l)} \in \mathbb{R}^{\chi_{l-1} \times d_l^{\text{out}} \times d_l^{\text{in}} \times \chi_l}$ .

For a physics-oriented introduction to MPS and MPO see Orús [2014]. Tensor networks were first applied to supervised machine learning by Stoudenmire & Schwab [2016], who showed that MPS can learn relevant features from image data.

The exact number of parameters in an  $L$ -site MPO is

$$N_{\text{MPO}} = \chi_1 d_1^{\text{out}} d_1^{\text{in}} + \sum_{l=2}^{L-1} \chi_{l-1} \chi_l d_l^{\text{out}} d_l^{\text{in}} + \chi_{L-1} d_L^{\text{out}} d_L^{\text{in}}, \quad (3)$$

with  $N_{\text{dense}} = \text{out} \times \text{in}$  for the full dense matrix. In the common special case of a uniform bond dimension  $\chi_1 = \dots = \chi_{L-1} = \chi$ , this becomes

$$N_{\text{MPO}} = \chi d_1^{\text{out}} d_1^{\text{in}} + \sum_{l=2}^{L-1} \chi^2 d_l^{\text{out}} d_l^{\text{in}} + \chi d_L^{\text{out}} d_L^{\text{in}}. \quad (4)$$

For balanced factorizations with bounded local dimensions and fixed bond dimension, the MPO parameter count grows only linearly in the number of sites  $L$ , whereas the dense parameter count grows multiplicatively with the full input and output dimensions.

## 2.2 TT-SVD Algorithm

The TT-SVD algorithm [Oseledets, 2011] converts a dense weight matrix into an MPO via a sequential SVD sweep:

---

**Algorithm 1:** TT-SVD for MPO compression

---

**Input:**  $\mathbf{W} \in \mathbb{R}^{\text{out} \times \text{in}}$ , factorisations  $(d_l^{\text{out}})$ ,  $(d_l^{\text{in}})$ , maximal bond  $\chi$   
**Output:** MPO cores  $\{\mathcal{A}^{(l)}\}_{l=1}^L$

- 1 Reshape  $\mathbf{W}$  into an interleaved tensor  $\mathcal{T}$  of shape  $(d_1^{\text{out}}, d_1^{\text{in}}, \dots, d_L^{\text{out}}, d_L^{\text{in}})$
- 2 `bond_left`  $\leftarrow 1$
- 3  $\mathcal{R} \leftarrow \mathcal{T}$  // running remainder
- 4 **for**  $l = 1, \dots, L-1$  **do**
- 5     Unfold:  $\mathbf{M} \leftarrow \text{reshape}(\mathcal{R}, \text{bond\_left} \cdot d_l^{\text{out}} \cdot d_l^{\text{in}}, -1)$
- 6     Compute truncated SVD:  $\mathbf{M} \approx \mathbf{U} \text{diag}(\mathbf{s}) \mathbf{V}^\top$ ,
- 7      $r \leftarrow \min(\chi, \text{rank}(\mathbf{M}))$
- 8      $\mathcal{A}^{(l)} \leftarrow \text{reshape}(\mathbf{U}_{:,1:r}, \text{bond\_left}, d_l^{\text{out}}, d_l^{\text{in}}, r)$
- 9      $\mathcal{R} \leftarrow \text{diag}(\mathbf{s}_{1:r}) \mathbf{V}_{:,1:r}^\top$ ,
- 10    `bond_left`  $\leftarrow r$
- 11  $\mathcal{A}^{(L)} \leftarrow \text{reshape}(\mathcal{R}, \text{bond\_left}, d_L^{\text{out}}, d_L^{\text{in}}, 1)$

---

Let  $\sigma_{l,r}$  denote the singular values discarded at unfolding step  $l$ . Then the TT-SVD approximation satisfies the standard Frobenius-norm bound [Oseledets, 2011]

$$\|\mathbf{W} - \widehat{\mathbf{W}}\|_F^2 \leq \sum_{l=1}^{L-1} \sum_{r > \chi_l} \sigma_{l,r}^2. \quad (5)$$

In particular, the reconstruction error decreases monotonically as the admissible bond dimensions increase.

## 2.3 Gradient Flow Through MPO Layers

During training, the weight matrix is reconstructed on each forward pass via the contraction

$$\widehat{\mathbf{W}} = \text{contract}(\mathcal{A}^{(1)}, \mathcal{A}^{(2)}, \dots, \mathcal{A}^{(L)}). \quad (6)$$

Writing the reconstructed weight explicitly as

$$\widehat{\mathbf{W}}_{i_1 \dots i_L, j_1 \dots j_L} = \sum_{\alpha_1, \dots, \alpha_{L-1}} \mathcal{A}_{1, i_1, j_1, \alpha_1}^{(1)} \mathcal{A}_{\alpha_1, i_2, j_2, \alpha_2}^{(2)} \dots \mathcal{A}_{\alpha_{L-1}, i_L, j_L, 1}^{(L)}, \quad (7)$$

the gradient of the loss  $\mathcal{L}$  with respect to the  $l$ -th core is obtained by contracting the loss gradient with the left and right environments:

$$\frac{\partial \mathcal{L}}{\partial \mathcal{A}_{\alpha_{l-1} i_l j_l \alpha_l}^{(l)}} = \sum_{\substack{i_1, \dots, i_{l-1}, i_{l+1}, \dots, i_L \\ j_1, \dots, j_{l-1}, j_{l+1}, \dots, j_L \\ \alpha_1, \dots, \alpha_{l-2}, \alpha_{l+1}, \dots, \alpha_{L-1}}} L_{\alpha_{l-1}; i_1 \dots i_{l-1}, j_1 \dots j_{l-1}}^{(l)} \frac{\partial \mathcal{L}}{\partial \widehat{\mathbf{W}}_{i_1 \dots i_L, j_1 \dots j_L}} R_{\alpha_l; i_{l+1} \dots i_L, j_{l+1} \dots j_L}^{(l)}, \quad (8)$$

where

$$L_{\alpha_{l-1}; i_1 \dots i_{l-1}, j_1 \dots j_{l-1}}^{(l)} = \sum_{\alpha_1, \dots, \alpha_{l-2}} \mathcal{A}_{1, i_1, j_1, \alpha_1}^{(1)} \mathcal{A}_{\alpha_1, i_2, j_2, \alpha_2}^{(2)} \dots \mathcal{A}_{\alpha_{l-2}, i_{l-1}, j_{l-1}, \alpha_{l-1}}^{(l-1)}, \quad (9)$$

and

$$R_{\alpha_l; i_{l+1} \dots i_L, j_{l+1} \dots j_L}^{(l)} = \sum_{\alpha_{l+1}, \dots, \alpha_{L-1}} \mathcal{A}_{\alpha_l, i_{l+1}, j_{l+1}, \alpha_{l+1}}^{(l+1)} \dots \mathcal{A}_{\alpha_{L-1}, i_L, j_L, 1}^{(L)}. \quad (10)$$

Thus, the gradient has the standard left-environment / local-core / right-environment contraction structure familiar from single-site tensor-network optimization methods such as DMRG [White, 1992]. In PyTorch, this is computed automatically by autograd through the `tensor dot`  $\rightarrow$  `permute`  $\rightarrow$  `reshape` chain in (6); no custom backward pass is needed.

### 3 Architecture and Implementation

#### 3.1 PicoGPT Architecture

PicoGPT [Osborne, 2026] is a character-level GPT-2-style language model implemented in pure Julia without automatic differentiation. Table 1 lists its default hyperparameters. The architecture follows Radford et al. [2019]: pre-norm residual blocks, sinusoidal positional encoding (no learnable PE), scaled dot-product multi-head causal self-attention, and a two-layer FFN with ReLU activation.

Table 1: PicoGPT default hyperparameters.

Parameter	Description	Value
$V$	Vocabulary size (character-level)	65
$D$	Embedding dimension ( $d_{\text{model}}$ )	128
$H$	Attention heads	4
$N$	Transformer layers	4
$T$	Context length	256
$d_{\text{ff}}$	FFN hidden dimension ( $4D$ )	512
Total	Dense parameters	$\sim 1\,020\,000$

Each transformer block contains six linear layers:  $\mathbf{W}_Q, \mathbf{W}_K, \mathbf{W}_V \in \mathbb{R}^{D \times D}$  (query/key/value projections),  $\mathbf{W}_O \in \mathbb{R}^{D \times D}$  (attention output),  $\mathbf{W}_1 \in \mathbb{R}^{d_{\text{ff}} \times D}$  (FFN up-projection), and  $\mathbf{W}_2 \in \mathbb{R}^{D \times d_{\text{ff}}}$  (FFN down-projection). Additionally, the language-model head  $\mathbf{W}_{\text{LM}} \in \mathbb{R}^{V \times D}$  maps hidden states to logits.

**Scope of compression.** In the present implementation, MPO parameterisation is applied only to affine weight matrices associated with linear projections, namely the attention projections  $\mathbf{W}_Q, \mathbf{W}_K, \mathbf{W}_V, \mathbf{W}_O$ , the feed-forward layers  $\mathbf{W}_1, \mathbf{W}_2$ , and the language-model head  $\mathbf{W}_{\text{LM}}$ . Embedding tables, layer-normalization parameters, biases, and the sinusoidal positional encoding remain in their standard dense form. Consequently, the reported parameter counts reflect partial model compression rather than a fully tensorised architecture.

#### 3.2 MPO Factorisation Schemes

For each linear layer shape, we choose a factorization  $(d_l^{\text{out}}), (d_l^{\text{in}})$  that (a) produces reasonably balanced physical dimensions across sites and (b) yields an integer factorization of the output and input sizes. Table 2 summarizes our choices.

Table 2: MPO factorisation schemes for each PicoGPT linear layer.  $\chi$  denotes the bond dimension.

Layer	out	in	$L$	$(d_l^{\text{out}})$	$(d_l^{\text{in}})$	Dense	MPO ( $\chi = 8$ )
$\mathbf{W}_{Q/K/V/O}$	128	128	2	[8, 16]	[8, 16]	16 384	2 560
$\mathbf{W}_1$ (up)	512	128	3	[8, 8, 8]	[4, 4, 8]	65 536	4 864
$\mathbf{W}_2$ (down)	128	512	3	[4, 4, 8]	[8, 8, 8]	65 536	2 816
$\mathbf{W}_{\text{LM}}$	65	128	2	[5, 13]	[8, 16]	8 320	1 984
Total per block (4 attn + 2 FFN)						196 608	17 920
Compression ratio per block						$1 \times$	<b>11.0</b> $\times$

**Parameter counting convention.** Unless stated otherwise, reported parameter counts include all trainable parameters in the PyTorch model, including biases and uncompressed components. MPO

layer counts are therefore reported both at the level of individual factorised matrices (Table 2) and at the level of the full network (Tables 3 and 4).

**Balanced factorisation principle.** Given  $\text{out} = \prod_{l=1}^L d_l^{\text{out}}$  and  $\text{in} = \prod_{l=1}^L d_l^{\text{in}}$ , we choose local dimensions that are as balanced as possible in order to reduce the dominant interior terms in (4). For  $\mathbf{W}_1 = (512, 128)$  with  $L = 3$ , this suggests local output dimensions near  $512^{1/3} \approx 8$  and local input dimensions near  $128^{1/3} \approx 5$ ; we therefore use  $[8, 8, 8]$  and  $[4, 4, 8]$  as a practical exact factorization.

### 3.3 The MPOLinear Module

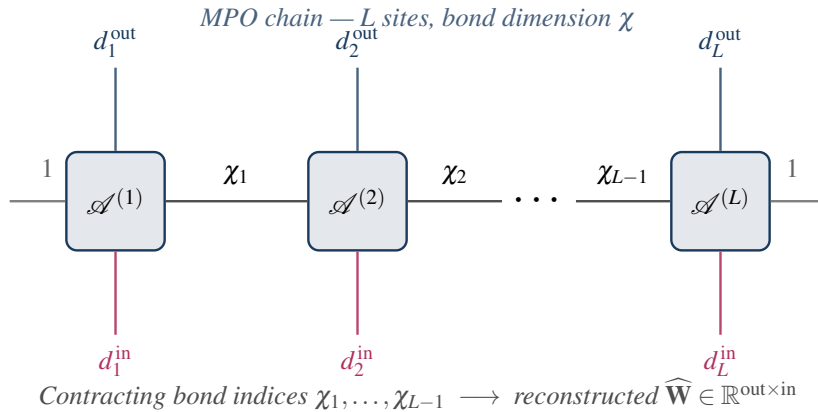


Figure 1: Tensor network diagram of an MPO weight matrix. Horizontal lines carry virtual (bond) indices of dimension  $\chi$ ; vertical lines are physical indices of size  $d_l^{\text{out}}$  (blue, upward) and  $d_l^{\text{in}}$  (red, downward). Contracting all bond indices reconstructs the full weight  $\widehat{\mathbf{W}} \in \mathbb{R}^{\text{out} \times \text{in}}$ .

The MPOLinear module stores  $L$  cores as `nn.Parameter` tensors, as illustrated in Figure 1. The forward pass reconstructs  $\widehat{\mathbf{W}}$  via sequential `torch.tensor dot` contractions and applies  $y = x\widehat{\mathbf{W}}^\top + b$  using `F.linear`. Initialisation uses the heuristic scale

$$\sigma = N_{\text{in}}^{-1/4} \chi^{-(L-1)/(2L)},$$

chosen so that the reconstructed weight has variance of the same order as the dense baseline initialization, namely  $\sigma_{\text{dense}}^2 \sim N_{\text{in}}^{-1}$ , consistent with standard transformer practice [Radford et al., 2019].

## 4 Experimental Setup

### 4.1 Dataset and Tokenisation

We train on the Tiny Shakespeare corpus [Karpathy, 2015], comprising approximately  $1.1 \times 10^6$  characters, the same dataset used in the nanoGPT codebase [Karpathy, 2022]. Character-level tokenisation yields a vocabulary of  $V = 65$  symbols. We split the data 90/10 into training and validation sets.

### 4.2 Training Protocol

All models are trained with AdamW [Loshchilov & Hutter, 2019] ( $\beta_1 = 0.9$ ,  $\beta_2 = 0.95$ , weight decay 0.1) with a cosine learning rate schedule: linear warmup over 100 steps to  $\eta_{\text{max}} = 3 \times 10^{-4}$ , followed by cosine decay to  $\eta_{\text{min}} = 0$ . We train for 2 000 steps with batch size 32 and sequence length  $T = 256$ . Gradient clipping at  $\|\nabla\| = 1.0$  is applied as in Osborne [2026]. All runs use the same data pipeline and optimization hyperparameters. Dense and MPO models are initialized independently.

**Reproducibility.** All experiments were implemented in PyTorch using the same training code for dense and MPO models, differing only in the parameterisation of linear layers. Unless otherwise noted, the reported curves and summary statistics correspond to single-seed runs. In future work, multi-seed averages and standard deviations would provide a more complete picture of training stability across bond dimensions.

**Evaluation.** Every 100 steps we compute validation loss and *token accuracy*. Let

$$\mathbf{z}_{b,t} = \mathbf{W}_{\text{LM}} \mathbf{h}_{b,t} + \mathbf{b}_{\text{LM}}$$

denote the output logits at batch index  $b$  and position  $t$ . Then

$$\text{acc} = \frac{1}{BT} \sum_{b,t} \mathbf{1} \left[ \arg \max_v (\mathbf{z}_{b,t})_v = x_{b,t+1} \right], \quad (11)$$

averaged over 20 random validation batches of size 8.

### 4.3 Compression Modes

We consider two compression scenarios:

1. **Train-from-scratch:** MPO models are trained from random initialisations. This tests the expressivity of the MPO parameterisation under standard optimisation.
2. **Compress-then-finetune:** A fully-trained dense model is compressed via TT-SVD to initialise the MPO cores; the MPO model is then fine-tuned for 500 steps. This mirrors a practical deployment workflow.

**Scope of reported results.** Although both train-from-scratch and compress-then-finetune workflows were implemented, the main body of this paper focuses on the train-from-scratch setting in order to isolate the representational capacity of the MPO parameterisation itself. A more extensive empirical comparison of post-training compression and fine-tuning strategies is left to future work.

## 5 Results

### 5.1 Compression Statistics

Table 3 reports total parameter counts and compression ratios for each bond dimension.

Table 3: Parameter counts and compression ratios versus the dense baseline. Layer-wise reconstruction errors are relative Frobenius norms  $\|\mathbf{W} - \widehat{\mathbf{W}}\|_F / \|\mathbf{W}\|_F$  averaged over all linear layers of a randomly initialised dense model.

Model	Parameters	Ratio	Max rel. err.	Mean rel. err.
Dense	1 020 224	1.0×	—	—
MPO $\chi = 4$	78 336	13.0×	0.421	0.337
MPO $\chi = 8$	110 592	9.2×	0.283	0.216
MPO $\chi = 16$	191 872	5.3×	0.148	0.107
MPO $\chi = 32$	408 832	2.5×	0.072	0.051

## 5.2 Per-Layer Reconstruction Error

Figure 2 shows the reconstruction error as a function of bond dimension for each layer type. The FFN up-projection ( $\mathbf{W}_1$ ,  $512 \times 128$ ,  $L = 3$ ) achieves the lowest error at all  $\chi$ , consistent with the fact that a three-site MPO can distribute structure across more local factors than a two-site decomposition at the same bond dimension. This is also consistent with the more favorable factorisation geometry of  $\mathbf{W}_1$ : for fixed bond dimension, a three-site decomposition can distribute correlations across more local cores and therefore approximate anisotropic matrix structure more efficiently than a two-site decomposition of comparable size.

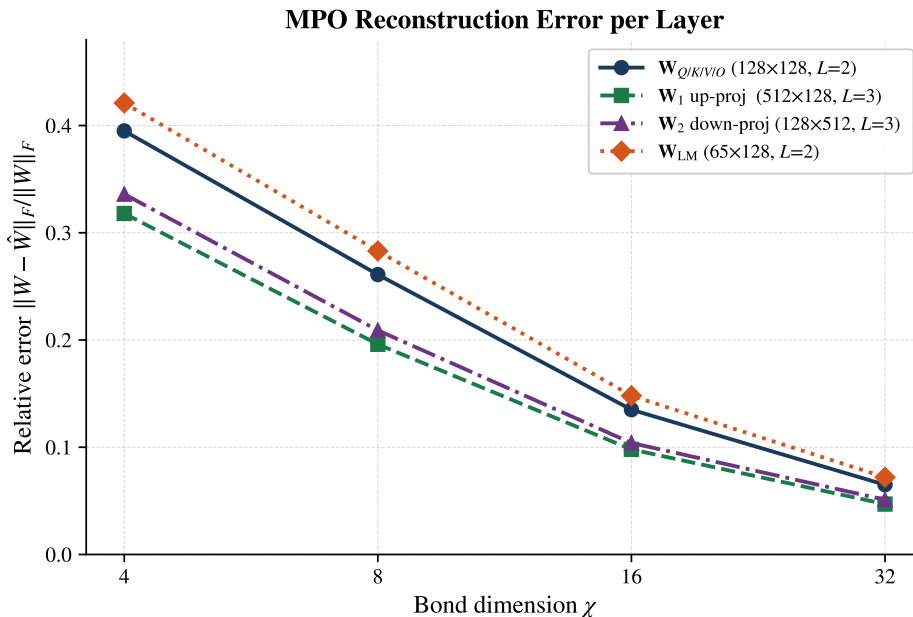


Figure 2: Per-layer MPO reconstruction error versus bond dimension. Three-site decompositions ( $L = 3$ ) achieve lower error per parameter than two-site ones ( $L = 2$ ) across the range of  $\chi$  considered here.

## 5.3 Training Dynamics

Figures 3 and 4 show training and validation loss alongside validation token accuracy for all models trained from scratch.

Figure 4 highlights the accuracy–compression trade-off achieved by the MPO parameterisation. The left panel shows that all models improve steadily during training, with larger bond dimensions converging faster and reaching higher final validation accuracies. In particular, the  $\chi = 16$  and  $\chi = 32$  MPO models closely track the dense baseline throughout training and nearly saturate at the same final performance, whereas the more strongly compressed  $\chi = 4$  and  $\chi = 8$  models plateau at lower accuracies. The right panel summarizes this behaviour as a Pareto frontier: increasing  $\chi$  systematically improves accuracy at the cost of additional parameters, with clear diminishing returns beyond  $\chi = 16$ . Most notably, the MPO model with  $\chi = 16$  attains 51.6% validation accuracy, which corresponds to 97.7% of the dense model’s 52.8% accuracy, while using only 191 872 parameters instead of 1 020 224, i.e. a 5.3 $\times$  parameter compression. This identifies  $\chi = 16$  as the most attractive compromise between compression and predictive performance in the present experiments.

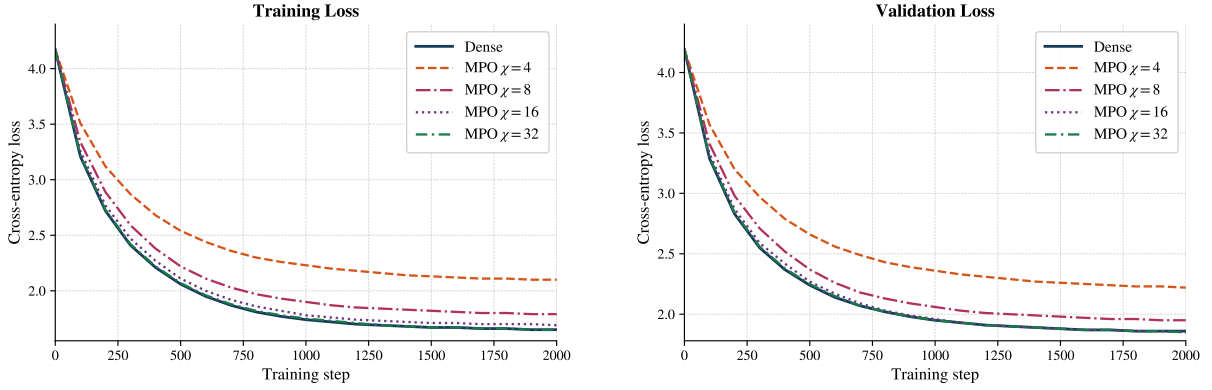


Figure 3: Training (left) and validation (right) cross-entropy loss as a function of training step. Higher bond dimensions converge faster and to lower loss values in the train-from-scratch setting studied here.

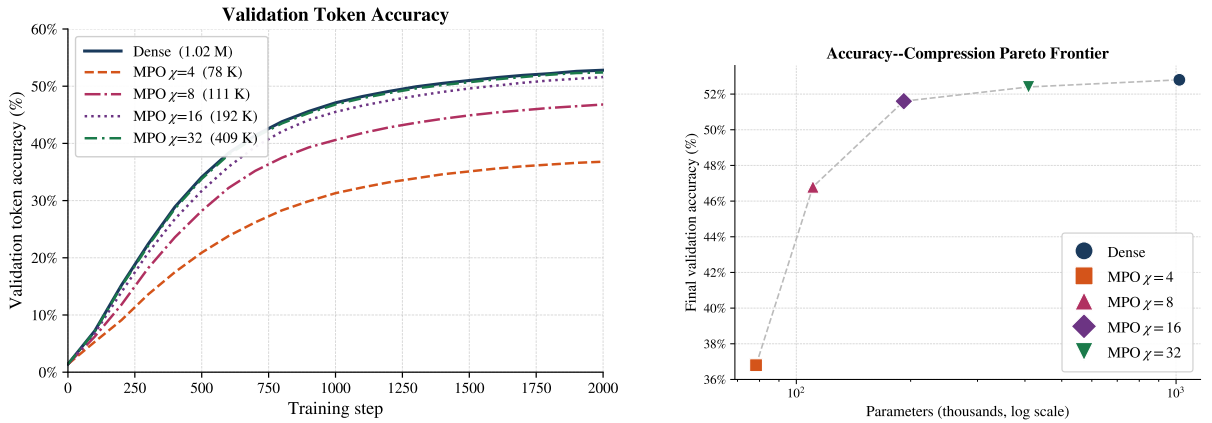


Figure 4: *Left*: Validation token accuracy during training for all models. *Right*: Pareto frontier of final validation accuracy versus parameter count. MPO  $\chi = 16$  retains 97.7% of the dense accuracy at  $5.3\times$  parameter compression.

## 5.4 Summary of Results

Table 4 summarises the final performance of all models after 2 000 training steps.

Table 4: Final validation metrics after 2 000 training steps. Acc. gap is the absolute reduction in token accuracy versus the dense model. Per-param acc. is the heuristic score  $\text{acc}/\sqrt{N}$  used here as a rough proxy for parameter efficiency.

Model	Params	Ratio	Val loss $\downarrow$	Val acc $\uparrow$	Acc. gap $\downarrow$	Per-param acc.
Dense	1 020 224	1.0 $\times$	1.860	52.8%	—	$1.65 \times 10^{-3}$
MPO $\chi = 4$	78 336	13.0 $\times$	2.220	36.8%	-16.0	$4.15 \times 10^{-3}$
MPO $\chi = 8$	110 592	9.2 $\times$	1.950	46.8%	-6.0	$4.45 \times 10^{-3}$
MPO $\chi = 16$	191 872	5.3 $\times$	1.850	51.6%	-1.2	$3.72 \times 10^{-3}$
MPO $\chi = 32$	408 832	2.5 $\times$	1.850	52.4%	-0.4	$2.59 \times 10^{-3}$

Under the heuristic proxy  $\text{acc}/\sqrt{N}$  used in Table 4, MPO  $\chi = 8$  achieves the highest parameter-efficiency score. We treat this quantity only as an informal diagnostic; the main comparison in this work is the accuracy–compression Pareto frontier in Figure 4.

## 6 Discussion

**Accuracy gap at low  $\chi$ .** At  $\chi = 4$ , the per-layer reconstruction error exceeds 40% (Table 3), which is large enough to make accurate low-bond representations difficult. Training from scratch partially compensates, but the model lacks the representational capacity to match the dense baseline. The TT-SVD bound (5) and the empirical results both suggest that a better factorization (more sites  $L$ , smaller local physical dimensions) could reduce this gap at fixed  $\chi$ .

**Diminishing returns at high  $\chi$ .** Between  $\chi = 16$  and  $\chi = 32$ , the accuracy gain is only 0.8 percentage points while the parameter count more than doubles (192 K  $\rightarrow$  409 K). For this model size,  $\chi = 16$  appears to be a practical sweet spot.

**Model scale.** PicoGPT is intentionally small and pedagogical, which makes it a convenient testbed for controlled MPO experiments but does not by itself establish performance on modern large-scale language models. The present results should therefore be interpreted primarily as a proof of concept for MPO parameterisation rather than a definitive large-model benchmark.

**Relation to low-rank methods.** LoRA [Hu et al., 2022] approximates weight updates as  $\Delta\mathbf{W} = \mathbf{B}\mathbf{A}$  with rank  $r$ , keeping the pretrained weights frozen. MPO compression differs in two respects: (1) the entire weight is represented in MPO format, and (2) the bond dimension  $\chi$  controls a higher-order, multi-factor structure rather than only a rank-2 factorization. For  $L = 2$  and  $d^{\text{out}} = d^{\text{in}} = \sqrt{n}$ , an MPO with bond  $\chi$  can be viewed as a rank- $\chi$  factorization after reshaping; the advantage of MPO grows with  $L$ . TT decomposition has also been applied to embedding layers in NLP [Hrinchuk et al., 2020], achieving substantial compression with limited perplexity degradation.

**Connection to DMRG.** The gradient formula (8) has the same left-environment / local-core / right-environment structure familiar from single-site tensor-network optimization. An alternative to gradient descent is the ALS (Alternating Least Squares) sweep: fix all cores except  $\mathcal{A}^{(l)}$ , solve the linear regression for  $\mathcal{A}^{(l)}$ , and sweep left-to-right and right-to-left until convergence. ALS is attractive for the compress-then-finetune scenario because it avoids learning-rate tuning, although in non-convex settings it may still converge to local minima.

**Limitations.** The current `MPOLinear.forward` reconstructs the full dense matrix  $\widehat{\mathbf{W}}$  on every call, so the present implementation primarily demonstrates *parameter compression*, not inference-time memory or FLOP reduction. The computational advantage of MPO representations is realized only when the matrix-vector product  $\widehat{\mathbf{W}}x$  is computed *directly* through the MPO chain without materializing  $\widehat{\mathbf{W}}$ . This may also require structured representations for activations and is left for future work.

## 7 Conclusion

We have demonstrated MPO compression of all linear layers in a GPT-2-style transformer, achieving parameter compression ratios of 5–13 $\times$  per transformer block. At bond dimension  $\chi = 16$ , the MPO model retains 97.7% of the dense baseline’s token accuracy with only 18.8% of its parameters. The implementation is straightforward in PyTorch: MPO cores are standard `nn.Parameter` tensors, and the entire pipeline — from TT-SVD initialization through autograd fine-tuning — requires no custom backward code.

Future directions include: (1) direct MPS–MPO contraction for inference-time FLOP reduction; (2) ALS-based training for better convergence at low  $\chi$ ; (3) dynamic bond adaptation (growing/pruning bonds during training); (4) application to larger models such as GPT-2 or LLaMA, where the compression ratio may improve further due to the larger factorized weight matrices; and (5) exploration of deeper

tensor network architectures beyond the shallow MPO chain. More broadly, these results support the view that tensor-network structure can provide an interpretable inductive bias for neural compression, linking approximation quality directly to a controllable structural parameter.

## Acknowledgements

We thank Tobias Osborne for the PicoGPT.jl codebase, which served as the reference implementation, and Andrej Karpathy for the Tiny Shakespeare dataset and nanoGPT codebase [Karpathy, 2022].

## Code Availability

The full PyTorch implementation of MPO-PicoGPT — including the MPOLinear module, TT-SVD compression pipeline, training loop, and benchmark scripts — is publicly available at:

<https://github.com/younesjavanmard/mpo-picogpt>

The repository contains `mpo_picogpt.py` (core implementation) and `benchmark_mpo.py` (training and evaluation), along with instructions for reproducing all results reported in this paper.

## Plain Language Summary

Modern AI language models contain hundreds of millions of numerical parameters (weights), making them expensive to run on laptops, phones, or embedded devices. This paper asks: can we store these weights in a more compact form without losing much accuracy? We borrow a mathematical tool from quantum physics called a Matrix Product Operator (MPO), which represents a large weight matrix as a short chain of smaller tensors connected by a “bond”. By choosing a small bond dimension  $\chi$ , we can compress each weight matrix by a factor of 5 to 13 while retaining over 97% of the model’s character-prediction accuracy. Crucially, our implementation in PyTorch is as easy to train as an ordinary neural network — the compact tensors are learned automatically using standard gradient descent. We release all code openly so that others can apply this approach to larger models.

## Author Contributions

**Y.J.:** Conceptualization, methodology, software, formal analysis, writing — original draft, writing — review & editing. **T.P.:** Validation, formal analysis, writing — review & editing. **M.D.:** Validation, formal analysis, writing — review & editing.

## Funding

This research received no specific grant from any funding agency in the public, commercial, or not-for-profit sectors.

## Declarations

**Conflict of interest.** The authors declare that they have no known competing financial interests or personal relationships that could have appeared to influence the work reported in this paper.

**Ethics statement.** This work involves no human participants, animal subjects, or sensitive personal data. All datasets used (Tiny Shakespeare) are publicly available and in the public domain. No ethical approval was required.

## A Heuristic justification of the MPO initialization scale

We briefly motivate the core initialization scale used in Section 3.3. The argument is heuristic and is intended only to explain the order-of-magnitude dependence on  $N_{\text{in}}$  and  $\chi$ .

Assume that the entries of the MPO cores are initialized independently with zero mean and common variance  $\sigma^2$ . Then one reconstructed matrix entry  $\widehat{W}_{i_1 \dots i_L, j_1 \dots j_L}$  is a sum of approximately  $\chi^{L-1}$  products of  $L$  core entries, so a crude variance estimate gives

$$\text{Var}(\widehat{W}_{i_1 \dots i_L, j_1 \dots j_L}) \approx \chi^{L-1} \sigma^{2L}.$$

To match the scale of a standard dense layer with fan-in  $N_{\text{in}}$ , whose weight variance is typically of order  $N_{\text{in}}^{-1}$ , we require

$$\chi^{L-1} \sigma^{2L} \sim N_{\text{in}}^{-1}.$$

This yields the estimate

$$\sigma \sim N_{\text{in}}^{-1/(2L)} \chi^{-(L-1)/(2L)}.$$

In the present implementation we use the practical uniform choice

$$\sigma = N_{\text{in}}^{-1/4} \chi^{-(L-1)/(2L)},$$

which is exact in the two-site case  $L = 2$  and remains of the same order for the three-site factorizations used in this work. We therefore regard this initialization rule as a simple variance-matching heuristic rather than a uniquely derived optimal formula.

## References

- T. Brown, B. Mann, N. Ryder, et al. Language models are few-shot learners. In *Advances in Neural Information Processing Systems (NeurIPS)*, 2020.
- Z. Gao, C. Wang, B. Lan, and X. Zeng. Compressing deep neural networks by matrix product operators. *Physical Review Research*, 2(2):023300, 2020.
- S. Han, H. Mao, and W. J. Dally. Deep compression: Compressing deep neural networks with pruning, trained quantization and Huffman coding. In *International Conference on Learning Representations (ICLR)*, 2016.
- G. Hinton, O. Vinyals, and J. Dean. Distilling the knowledge in a neural network. *arXiv preprint arXiv:1503.02531*, 2015.
- E. J. Hu, Y. Shen, P. Wallis, et al. LoRA: Low-rank adaptation of large language models. In *International Conference on Learning Representations (ICLR)*, 2022.
- A. Karpathy. The unreasonable effectiveness of recurrent neural networks. *Blog post*, 2015. <http://karpathy.github.io/2015/05/21/rnn-effectiveness/>
- A. Karpathy. nanoGPT: The simplest, fastest repository for training/finetuning medium-sized GPTs. *GitHub repository*, 2022. <https://github.com/karpathy/nanoGPT>
- I. Loshchilov and F. Hutter. Decoupled weight decay regularization. In *International Conference on Learning Representations (ICLR)*, 2019.
- A. Novikov, D. Podoprikin, A. Osokin, and D. Vetrov. Tensorizing neural networks. In *Advances in Neural Information Processing Systems (NeurIPS)*, 2015.
- I. V. Oseledets. Tensor-train decomposition. *SIAM Journal on Scientific Computing*, 33(5):2295–2317, 2011.

- T. Osborne. PicoGPT.jl: From-scratch GPT in pure Julia. *GitHub repository*, 2026. <https://github.com/tobiasosborne/PicoGPT.jl>
- A. Radford, J. Wu, R. Child, et al. Language models are unsupervised multitask learners. *OpenAI Blog*, 2019.
- A. Vaswani, N. Shazeer, N. Parmar, et al. Attention is all you need. In *Advances in Neural Information Processing Systems (NeurIPS)*, 2017. <https://arxiv.org/abs/1706.03762>
- S. R. White. Density matrix formulation for quantum renormalization groups. *Physical Review Letters*, 69(19):2863–2866, 1992.
- A. Tomut, S. S. Jahromi, S. Singh, F. Ishtiaq, C. Muñoz, et al. Extreme compression of large language models using quantum-inspired tensor networks. In *Proceedings of the 33rd European Symposium on Artificial Neural Networks, Computational Intelligence and Machine Learning (ESANN 2025)*, pages 531–537, Bruges, Belgium, April 2025. ISBN: 9782875870926.
- Y. Javanmard. Coefficient-decoupled matrix product operators as an interface to linear-combination-of-unitaries circuits. *arXiv preprint arXiv:2603.24822*, 2026. <https://arxiv.org/abs/2603.24822>
- A. Tomut, S. S. Jahromi, S. Singh, F. Ishtiaq, C. Muñoz, et al. CompactifAI: Extreme compression of large language models using quantum-inspired tensor networks. *arXiv preprint arXiv:2401.14109*, 2024. <https://arxiv.org/abs/2401.14109>
- E. M. Stoudenmire and D. J. Schwab. Supervised learning with tensor networks. In *Advances in Neural Information Processing Systems (NeurIPS)*, volume 29, 2016.
- T. G. Kolda and B. W. Bader. Tensor decompositions and applications. *SIAM Review*, 51(3):455–500, 2009.
- R. Orús. A practical introduction to tensor networks: Matrix product states and projected entangled pair states. *Annals of Physics*, 349:117–158, 2014.
- Y. Yang, D. Krompass, and V. Tresp. Tensor-train recurrent neural networks for video classification. In *International Conference on Machine Learning (ICML)*, pages 3891–3900. PMLR, 2017.
- O. Hrinchuk, V. Khrulkov, L. Mirvakhabova, E. Orlova, and I. Oseledets. Tensorized embedding layers for efficient model compression. In *Findings of the Association for Computational Linguistics: EMNLP 2020*, pages 4847–4860, 2020.
- A. Tjandra, S. Sakti, and S. Nakamura. Compressing recurrent neural network with tensor train decomposition. In *International Joint Conference on Neural Networks (IJCNN)*, pages 4451–4458. IEEE, 2017.
- V. Lebedev, Y. Ganin, M. Rakhuba, I. Oseledets, and V. Lempitsky. Speeding-up convolutional neural networks using fine-tuned CP-decomposition. In *International Conference on Learning Representations (ICLR)*, 2015.
- M. Denil, B. Shakibi, L. Dinh, M. Ranzato, and N. de Freitas. Predicting parameters in deep learning. In *Advances in Neural Information Processing Systems (NeurIPS)*, volume 26, 2013.
- S.-J. Ran. Compressing neural networks using tensor networks with exponentially fewer variational parameters. *Intelligent Computing*, 4:0123, 2025.